Journal of Marine Science and Application (2021) 20:325–332
https://doi.org/10.1007/s11804-021-00201-6

Adaptive Neural Observer-Based Nonsingular Super-Twisting Terminal Sliding-Mode Controller Design for a Class of Hovercraft Nonlinear Systems

Hamede Karami[1] · Reza Ghasemi[1]

Received: 7 July 2019 / Accepted: 5 September 2020 / Published online: 9 July 2021

Abstract
Designing a controller to stabilize maneuvering hovercrafts is an important challenge in amphibious vehicles. Hovercrafts are implemented in several applications, such as military missions, transportation, and scientific tasks. Thus, to improve their performance, it is crucial to control the system and compensate uncertainties and disruptions. In this paper, both classic and intelligent approaches are combined to design an observer-based controller. The system is assumed to be both controllable and observable. An adaptive neural network observer with guaranteed stability is derived for the nonlinear dynamics of a hovercraft, which is controlled via a nonsingular super-twisting terminal sliding-mode method. The main merits of the proposed method are as follows: (1) the Lyapunov stability of the overall closed-loop system, (2) the convergence of the tracking and observer errors to zero, (3) the robustness against uncertainties and disturbances, and (4) the reduction of the chattering phenomena. The simulation results validate the excellent performance of the derived method.

Keywords Hovercraft · Neural network · Observer · Terminal sliding mode · Nonlinear system · Nonsingular · Super twisting

1 Introduction

Hovercrafts, also known as air cushion vehicles (ACVs), are under actuated electromechanical vehicles that can move on water, land, and any kind of surface; this flexibility is due to the air cushion support underneath the vehicles, which minimizes friction with the bottom surface. Therefore, they are employed for applications such as helping flood refugees, transportation, and accessing impassable places (Rashid et al. 2012; Mutreja et al. 2015). Because of these extensive applications, it is crucial to control and solve the problems limiting these vehicles.

Article Highlights
- In order to overcome the unknown dynamical system, the adaptive neural network is derived.
- To reduce the chattering phenomena and the finite time convergence of the tracking error to neighborhood of zero are both guaranteed.
- To validate the proposed methodology, the controller is applied on the nonlinear model of hovercraft.

✉ Reza Ghasemi
R.ghasemi@qom.ac.ir; Reghasemi@gmail.com

[1] Department of Electrical Engineering, University of Qom, Qom 3716146611, Iran

In both the modeling and control phases, hovercrafts may face challenges such as the inaccessibility of the variable states and the disturbance effects on the motion performance (Soneda and Ohtsuka 2002; Morales et al. 2015). Various observers have been designed to observe unknown parameters (Soneda and Ohtsuka 2002; Rigatos and Raffo 2015) and disturbances (Jeong et al. 2015; Xie et al. 2018; Lin and Wang 2017). Furthermore, observer design for nonlinear systems is an important subject in control engineering, and much effort has been channeled toward designing more efficient and up-to-date observers (Niu et al. 2004; Qiu et al. 2019; Nath et al. 2019; Shah and Singh 2019; Huang et al. 2019; Liu and Li 2019).

In recent years, artificial intelligence based on artificial neural networks has been used in several industrial applications. In the same way, neural network observers are widely used for the estimation of disturbances and unknown system parameters (Lau et al. 2019; Zhao et al. 2019; Wang et al. 2018; Liu et al. 2018). This method has the advantages of parallelism during information processing, high accuracy with minimal neural units, and distributed knowledge representation (Resendiz et al. 2008; Grigoryev et al. 2010).

Artificial intelligence-based controllers that have been implemented on hovercrafts thus far include artificial neural network controllers and fuzzy controllers (Tunstel et al. 1994; Tanaka

et al. 2000; Wang et al. 2012; Duan et al. 2018). Some classic controllers include nonlinear Lyapunov-based tracking controller, PID controller, adaptive controller, and backstepping and second-order sliding-mode controller, which have been applied on hovercraft nonlinear systems (Aguiar et al. 2003; Marconett 2003; Wang et al. 2010; Ding et al. 2017; Sira-Ramírez 2002).

The nonsingular fast-terminal sliding-mode methodology based on an adaptive neural network disturbance observer has been applied on flexible air-breathing hypersonic vehicles (Ma et al. 2019), and its performance is superior to the backstepping strategy. Terminal sliding-mode control is robust in the presence of both bounded disturbances and uncertainties and can stabilize the system in finite time (Hui and Li 2009; Mobayen and Javadi 2017).

The chattering effect in the sliding-mode control simulates the fast dynamics of sensors and actuators. This phenomenon damages the system actuator; therefore, in this context, a super-twisting algorithm is considered to eliminate the chattering effect (Boiko and Fridman 2005; Utkin and Poznyak 2013).

The nonlinear characteristics of the system and disturbances are estimated through experimental data in a neural network, and the weights of the layers are adaptively adjusted. This approach can enhance system robustness against disturbances and uncertainties (Zhou et al. 2012; Mobayen et al. 2017; Abbaspour et al. 2017; Sharafian and Ghasemi 2017; Khoygani and Ghasemi 2016; Sharafian and Ghasemi 2019; Moghanloo and Ghasemi 2016).

Some finite-time control techniques that combine the fuzzy and cascade methods have been implemented for other marine vehicles. These methods also showed remarkable performance (Liang et al. 2019; Wang and He 2019; Wang and Ahn 2019).

The main contributions of the paper are the use of a neural observer-based sliding-mode control, which has not been previously reported, and the use of a super-twisting algorithm to reduce the chattering phenomena.

In this paper, the terminal sliding-mode controller is adopted to control the ACV. The nonlinear dynamics considered in this paper induces lateral forces on the ACV, depending on the torque. Compared with the other studies that rely on the measurability of states of the ACV, a sensorless approach is derived in this paper. The neural observer is designed to identify the nonlinearity with high accuracy and guarantee the convergence of the observer to zero. In addition, the terminal sliding-mode controller based on the proposed observer is developed to satisfy the closed-loop system stability.

2 Hovercraft Dynamic Model

2.1 Model Description

The nonlinear dynamics adopted in this paper has been derived and identified in Liang et al. (2019). The equations of velocity components as shown in Figure 1 are presented below:

$$\begin{cases} \dot{u} = -m^{-1}d_{u_0}\operatorname{sgn} u - m^{-1}d_u u + m^{-1}b_T T\cos\theta + vr \\ \dot{v} = -m^{-1}d_{v_0}\operatorname{sgn} v - m^{-1}d_v v + m^{-1}b_T T\sin\theta - ur \\ \dot{r} = -J^{-1}d_{r_0}\operatorname{sgn} r - J^{-1}d_r r - J^{-1}ab_T T\sin\theta \end{cases} \tag{1}$$

where u and v are the surge and sway velocities; r is the angular velocity; $\{d_{u0}, d_u, d_{v0}, d_v, d_{r0}, d_r\} \in R$ are the friction and drag coefficients; a is the length of the arm from the center of mass to the rudder surface; T is the thrust force; and θ is the rudder angle; the coefficient b_T scales the thrust input from [0, 1] to force in Newton.

The model is actuated by the thrust force T and rudder angle θ, which are generated by propellers subjected to velocity drag forces. In these equations, the lateral force is induced on the system dependent on the torque. By some mathematical manipulations and particularization, the torque is disregarded in the mentioned equations.

The kinematics equation is as follows:

$$\dot{\boldsymbol{P}} = \boldsymbol{RV} \tag{2}$$

where $\boldsymbol{P} = \begin{bmatrix} x \\ y \end{bmatrix} \in \mathbb{R}^2$ is the system position $\boldsymbol{P} = [x \ y]$, and $\boldsymbol{V} = [u \ v]^{\mathrm{T}} \in \mathbb{R}^2$ corresponds to the velocity. The rotation matrix R is as follows:

$$\boldsymbol{R} = \begin{bmatrix} \cos\theta & -\sin\theta \\ \sin\theta & \cos\theta \end{bmatrix} \tag{3}$$

By substituting (2) into (1), the kinematics and the overall dynamics of the hovercraft is obtained as follows:

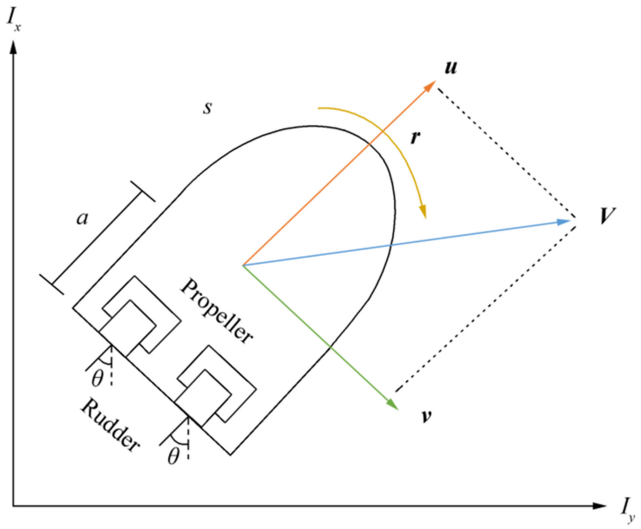

Figure 1 Sketch of air cushion vehicles model

$$\begin{cases} \begin{bmatrix} \dot{x} \\ \dot{y} \end{bmatrix} = \begin{bmatrix} \cos\theta & -\sin\theta \\ \sin\theta & \cos\theta \end{bmatrix} \begin{bmatrix} u \\ v \end{bmatrix} \\ \dot{u} = -m^{-1} d_{u_0} \operatorname{sgn} u - m^{-1} d_u u + m^{-1} b_T T \cos\theta + vr \\ \dot{v} = -m^{-1} d_{v_0} \operatorname{sgn} v - m^{-1} d_v v + m^{-1} b_T T \sin\theta - ur \\ \dot{r} = -J^{-1} d_{r_0} \operatorname{sgn} r - J^{-1} d_r r - J^{-1} a b_T T \sin\theta \end{cases} \tag{4}$$

2.2 Model Transportation

To design the controller, the dynamics mentioned in (4) should be standardized in the strict feedback form; the diffeomorphism transformation should satisfy the following equation:

$$\begin{cases} z_1 = T_1(x) \\ z_2 = \dfrac{\partial T_1}{\partial x}\dot{x} + \dfrac{\partial T_1}{\partial y} y \end{cases} \tag{5}$$

After some mathematical manipulations, a new state space is obtained as Eq. (6):

$$\begin{cases} z_1 = T_1(x) = u^2 + v^2 \\ z_2 = \dot{T}_2(x) = \dot{z_1} \end{cases} \tag{6}$$

where $z_1 = T_1(x) = u^2 + v^2$ and $z_2 = \dot{T}_2(x) = \dot{z_1}$ are the transformations between the model in Eq. (4) and the equation below.

To better describe the system, Eqs. (6) and (4) can be rewritten as Eq. (7):

$$\begin{cases} \dot{\boldsymbol{z_1}} = \boldsymbol{z_2} \\ \dot{\boldsymbol{z_2}} = \boldsymbol{f}(\boldsymbol{z}, \boldsymbol{U}) \end{cases} \tag{7}$$

where $f(z, U) = 2u(-m^{-1} d_{v_0} \operatorname{sgn}(v) - m^{-1} d_v v + m^{-1} b_T T \sin\theta - ur) + 2v(-m^{-1} d_{u_0} \operatorname{sgn}(u) - m^{-1} d_u u + m^{-1} b_T T \cos\theta + vr)$, and u demonstrates the inputs of the system containing (θ, T), and z refers to $[\, z_1 \quad z_2 \,]^{\mathrm{T}}$.

The general equation of the system is considered as follows:

$$\begin{cases} \dot{\boldsymbol{z}}(\boldsymbol{t}) = \boldsymbol{f}(\boldsymbol{z}, \boldsymbol{U}) \\ \boldsymbol{Y}(\boldsymbol{t}) = \boldsymbol{C}\boldsymbol{z}(\boldsymbol{t}) \end{cases} \tag{8}$$

By adding and subtracting $\boldsymbol{A}z(t)$ to $f(z,U)$, Eq. (8) becomes:

$$\begin{cases} \dot{\boldsymbol{z}}(\boldsymbol{t}) = \boldsymbol{G}(\boldsymbol{z}, \boldsymbol{U}) + \boldsymbol{A}\boldsymbol{z}(\boldsymbol{t}) \\ \boldsymbol{Y}(\boldsymbol{t}) = \boldsymbol{C}\boldsymbol{z}(\boldsymbol{t}) \end{cases} \tag{9}$$

where A is a Hurwitz matrix and $G(z, U) = f(z, U) - Az(t)$; $G(z, U)$ contains both the uncertainty nonlinear and disturbance terms.

Without loss of generality, the following assumptions are considered:

Assumption 1:
Uncertainties that exhibit time dependence are omitted.
Assumption 2: (A, C) is observable.

3 Neural State Observer Design

3.1 Neural Network Observer Structure

Both the states and the inputs enter the neural network input layer. There are two input neurons. The hidden layer has three neurons and the output layer has two. The neuron numbers of the hidden layer are obtained by checking the neural network model response. The activation functions of the hidden layer and the output layer are considered a bounded hyperbolic tangent. The weights of the neurons are updated by the backpropagation algorithm: a neural network–based method that calculates the gradient of the error with respect to the weights for given inputs by propagating the error backward. The proposed algorithm considers the initial values as random small numbers around zero. The optimal parameters are used to estimate unavailable states.

In Figure 2, the control input is $U = U_{\mathrm{eq}} + U_r$, and the states are $\widehat{\boldsymbol{Z}} = [\, \widehat{z}_1 \quad \widehat{z}_2 \,]^{\mathrm{T}}$.

3.2 Observer Formulation

The proposed observer, which is considered in this approach, is defined as (10):

$$\left\{ \dot{\widehat{z}} = A\widehat{z} + \widehat{G}\left(\widehat{z}, U\right) + \Gamma\left(Y - C\widehat{z}\right) \widehat{Y} = C\widehat{z} \right. \tag{10}$$

where $\widehat{z}$ is the estimated state; $\widehat{Y}$ denotes the system output whose states are estimated; A and C are matrices, and the (A, C) pair is observable; $\Gamma \in \mathbb{R}^n$ is the observer gain to estimate the nonlinear term $G(z, U)$; it should be chosen such that $(A - \Gamma C)$ is Hurwitz. The neural network observer is proposed as follows:

$$G(z, U) = w^{\mathrm{T}} \varphi\left(w'^{\mathrm{T}} \overline{z}^{\mathrm{T}} \right) + \varepsilon \tag{11}$$

w, w' are the weights of the output and hidden layers; ε is the approximation error, which is bounded; $\overline{\boldsymbol{z}} = [z \; U]$; and the weight of first layer is $w' = I$ which is the approximation of the nonlinear function of (10) and is based on the neural network as the universal approximator; it is given by (11):

$$\widehat{G}(z, U) = \widehat{w}^{\mathrm{T}} \varphi\left(\overline{\widehat{z}} \right) \tag{12}$$

where $\widehat{w}$ is the weight estimation.

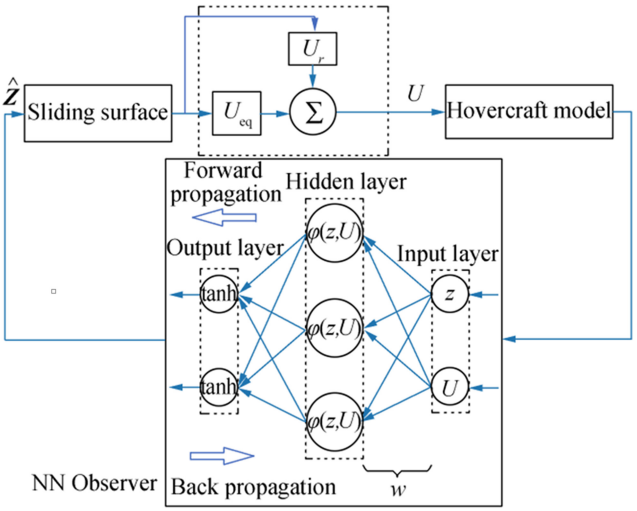

Figure 2 Proposed structure

The observer error is considered as $\tilde{z} = z - \hat{z}$; the observer error dynamics is obtained as follows:

$$\begin{cases} \dot{\tilde{z}} = A_c\tilde{z} + \tilde{w}\varphi\left(\hat{\bar{z}}\right) + W(t)\tilde{Y}(t) = C\tilde{z}(t) \end{cases} \tag{13}$$

where $\tilde{w} = w - \hat{w}$, $A_c = A - \Gamma C$; $W(t)$ is the disturbance term, which is bounded and obtained from (13); and $\boldsymbol{A}_c$ is a Hurwitz matrix.

$$w(t) = w\left[\varphi\left(\bar{z}\right) - \varphi\left(\hat{\bar{z}}\right)\right] + \varepsilon(z) \tag{14}$$

3.3 Stability of Observer

The stability of the neural observer is proved in this section by considering the weight updating mechanism.

Theorem 1 Consider the hovercraft model mentioned in (4) and the observer model derived in (9) that satisfies assumptions (1) to (3). The proposed neuro-observer based on the update laws as mentioned in Eq. (15) makes the states of the observer asymptotically converge to the system states, and the objective function ($J = 0.5\left(\tilde{Y}^{\mathrm{T}}\tilde{Y}\right)$) reaches its min point $J = 1/2\left(\tilde{Y}^{\mathrm{T}}\tilde{Y}\right)$.

$$\dot{\hat{w}} = -\ell\left(\tilde{Y}^{\mathrm{T}}CA_c^{-1}\right)^{\mathrm{T}}\left(\varphi\left(\hat{\bar{z}}\right)\right)^{\mathrm{T}} - \gamma\left\|C\tilde{z}\right\|\hat{w} \tag{15}$$

where the learning rate (ℓ) is positive and γ is a small positive number; then $\tilde{z}, \tilde{Y}, \tilde{w} \in L_\infty$.

Proof: Equation (15) can be rewritten as follows:

$$\dot{\tilde{w}} = \ell\left(\tilde{z}^{\mathrm{T}}C^{\mathrm{T}}CA_c^{-1}\right)^{\mathrm{T}}\left(\varphi\left(\hat{\bar{z}}\right)\right)^{\mathrm{T}} + \gamma\left\|C\tilde{z}\right\|\hat{w} \tag{16}$$

The Lyapunov function candidate is as follows:

$$L = \frac{1}{2}\tilde{z}^{\mathrm{T}}Q\tilde{z} + \frac{1}{2}\mathrm{tr}\left(\tilde{w}^{\mathrm{T}}\gamma^{-1}\tilde{w}\right) \tag{17}$$

where $Q = Q^{\mathrm{T}}$ is a positive definite matrix. $\boldsymbol{A}_c^{\mathrm{T}}\boldsymbol{Q} + \boldsymbol{Q}\boldsymbol{A}_c = -H$, and H is positive definite, and $\boldsymbol{A}_c$ is a Hurwitz matrix. $I3$ is a small positive constant, and $\mathrm{tr}(A^{\mathrm{T}}B) = BA^{\mathrm{T}}$. According to the Lyapunov function in (17), L is positive, and according to the Lyapunov theorem, $\dot{L}$ should be negative; therefore, based on the time derivative of the Lyapunov function, (18) is obtained:

$$\dot{L} = \frac{1}{2}\dot{\tilde{z}}^{\mathrm{T}}Q\tilde{z} + \frac{1}{2}\left(\tilde{z}^{\mathrm{T}}Q\dot{\tilde{z}}\right) + \frac{1}{2}\left(\tilde{w}^{T}\gamma^{-1}\dot{\tilde{w}}\right)^{\mathrm{T}} \tag{18}$$

Equations (13) and (16) are substituted into (18), and the following equation is obtained:

$$\begin{aligned}\dot{L} = &-\frac{1}{2}\tilde{z}^{\mathrm{T}}H\tilde{z} + \tilde{z}^{\mathrm{T}}Q\left(\tilde{w}\varphi\left(\hat{\bar{z}}\right) + w\right) \\ &+ \left(-\tilde{w}^{\mathrm{T}}\zeta\tilde{z}\varphi^{\mathrm{T}} + w + \tilde{w}^{\mathrm{T}}\left\|C\tilde{z}\right\|\left(w - \tilde{w}\right)\right)\end{aligned} \tag{19}$$

where $\zeta = \ell\gamma^{-1}\boldsymbol{A}_c^{-\mathrm{T}}C^{\mathrm{T}}C$.

Without loss of generality, Eqs. (20) and (21) are considered to prove the theorem.

$$\mathrm{tr}\left(\tilde{w}^{\mathrm{T}}\left(w - \tilde{w}\right)\right) \le k_1\|w\| - \left\|\tilde{w}\right\|^2 \tag{20}$$

$$\mathrm{tr}\left(\tilde{w}^{\mathrm{T}}\zeta\tilde{z}\varphi^{\mathrm{T}}\right) \le k_2\left\|\tilde{w}^{\mathrm{T}}\right\|\|\zeta\|\left\|\tilde{z}\right\| \tag{21}$$

where k_1 and k_2 are the upper bounds of the activation function and weight, respectively. Based on (20) and (21), Eq. (19) can be rewritten as:

$$\begin{aligned}\dot{L} \le &\left(-\frac{1}{2}\lambda_{\min}(H)\left\|\tilde{z}\right\|^2 + \left\|\tilde{z}\right\|\|Q\|\left(\left\|\tilde{w}\right\|k_2 + \overline{w}\right)\right. \\ &\left. + k_2\left\|\tilde{w}^{\mathrm{T}}\right\|\|\zeta\|\left\|\tilde{z}\right\| + \left(k_1\|w\| - \left\|\tilde{w}\right\|^2\right)\|C\|\left\|\tilde{z}\right\|\right.\end{aligned} \tag{22}$$

where $\lambda_{\min}(H)$ is the minimum H eigenvalues. If the squares of $\|\widetilde{w}\|$ is completed, then the negative definiteness of (22) is guaranteed in the following set:

$$\Omega = \left\{ z \middle| \begin{array}{c} \left\|\widetilde{z}\right\| \geq \left(2\|Q\|\overline{w} \right. \\ \left. + \frac{1}{2}\left(k_1\|Q\| + k_2\|C\| + k_1\|\zeta\|\right)^2\right)/\lambda_{\min}(H) \end{array} \right\} \quad (23)$$

The proof is completed.

4 Controller Design

4.1 Nonsingular Terminal Sliding-Mode Control

To design the nonsingular terminal sliding-mode controller, Eq. (20) is considered for the sliding surface:=

$$S = \widehat{z}_1 + \lambda \widehat{z}_2^{\frac{p}{q}} \quad (24)$$

where $\frac{1}{2} < \frac{p}{q} < 1$ and $\widehat{z}_1$ and $\widehat{z}_2$ are the states of dynamics, which are estimated by the observer.

The control input (U) should be considered in two components: the reaching phase and the sliding phase.

$$\begin{cases} \theta = \theta_r + \theta_{\text{eq}} \\ T = T_r + T_{\text{eq}} \end{cases} \quad (25)$$

where θ_r and T_r are the reaching phase inputs (rudder angle and thrust force) and θ_{eq} and T_{eq} are the sliding phase inputs. The reaching phase inputs are obtained from (26), and the super-twisting algorithm is used. The super-twisting algorithm increases the robustness of the control structure against uncertainties. Only the knowledge of the sign of the sliding variable during online operation is required (Kunusch et al. 2008)

$$\begin{cases} \theta_r = -\alpha_1 |S|^{\rho_1}\text{sign}(s) - \beta_1 \int \text{sign}(S)\text{d}t \\ T_r = -\alpha_2 |S|^{\rho_2}\text{sign}(s) - \beta_2 \int \text{sign}(S)\text{d}t \end{cases} \quad (26)$$

Based on the time derivative of the sliding surface (24) and substituting (26), the equivalent term of the thrust force in the sliding phase is derived as follows:

$$T_{\text{eq}} = \frac{\lambda p \widehat{z}_2^{\frac{p}{q}-1}}{q}\left(2u\left(m^{-1}d_{u_0}\text{sgn}(u) + m^{-1}d_u u\right) + 2v\left(m^{-1}d_{v_0}\text{sgn}(v) + m^{-1}d_v v\right)\right) - \widehat{z}_2 \quad (27)$$

Furthermore, the equivalent term of the rudder angle is as follows:

$$\theta_{\text{eq}} = \frac{q}{2\lambda b_T p v m^{-1}}\widehat{z}_2^{1-\frac{p}{q}} - \frac{u}{v} \quad (28)$$

Therefore, these control inputs are applied to the system, and the stabilities of the overall closed-loop system, the observer, and the controller are proved.

4.2 Stability Analysis

Theorem 2 Consider the hovercraft, which is described by (4) and satisfies assumptions 1 and 2, and the observer derived in (9) based on the learning laws (15). The nonsingular terminal sliding-mode controller with the candidate sliding surface (24) and control inputs (25)–(28) make the system asymptotically stable, and the signals involved in the closed-loop system remain bounded.

Proof The Lyapunov function candidate is as follows:

$$V = \frac{1}{2}S^2 \quad (29)$$

To prove the stability of the closed-loop system, the time derivative of (29) should satisfy the following inequality:

$$\dot{V} = S\dot{S} \leq -\eta|S| \quad (30)$$

By substituting (24) and its derivative into (30), the following equation is obtained:

$$\begin{aligned} \dot{V} &= S\left(\dot{\widehat{z}}_1 + \lambda\frac{p}{q}\widehat{z}_2^{\frac{p}{q}-1}\dot{\widehat{z}}_2\right) \\ &= S\left(\widehat{z}_2 + \lambda\frac{p}{q}\widehat{z}_2^{\frac{p}{q}-1}\left(2u\dot{u} + 2v\dot{v}\right)\right) \end{aligned} \quad (31)$$

Based on Eq. (10), (31) is rewritten as:

$$\dot{V} = S\left(\widehat{z}_2 + \lambda\frac{p}{q}\widehat{z}_2^{\frac{p}{q}-1}\left(2u\left(-m^{-1}d_{u_0}\text{sgn}(u) - m^{-1}d_u u + m^{-1}b_T T\cos\theta + vr\right) + 2v\left(m^{-1}d_{v_0}\text{sgn}(v) - m^{-1}d_v v + m^{-1}b_T T\sin\theta - ur\right)\right)\right) \quad (32)$$

Table 1 System and controller parameters

Parameter	Value	Parameter	Value
p	3	B	2
q	5	λ	10
ρ_1	1	m	0.585
ρ_2	1	a	0.14
α_1	0.0001	J	0.01
α_2	0.001	b_T	10
β_1	0.002	d_{u_0}	0.1
β_2	0.001	d_{v_0}	0.01
d_u	0.6	d_{r_0}	0.004
d_v	0.8	d_r	0.1

Based on the control input in (25) and $|S| = S\,\mathrm{sgn}(S)$, Eq. (32) becomes:

$$\dot{V} = -\alpha|S|^{\rho}\mathrm{sgn}(s) - \beta S\int \mathrm{sgn}(S)\mathrm{d}t \tag{33}$$

where α, ρ, and β are positive constants.

Through the control input mentioned in (25)–(28) and the application of some mathematical manipulations to (32), Eq. (33) leads to (34):

$$\dot{V} = -k|S| < -\eta\,|S| \rightarrow k > \eta \tag{34}$$

To satisfy Eq. (34), the inequality condition $k > \eta$ should be satisfied. Thus, the asymptotic stability of the system is proved and the proof is complete.

5 Simulation Result

The system was simulated using friction coefficients and system parameters in Liang et al. (2019) and Talebi et al. (2010). The controller, system, and observer parameters are presented in Table 1.

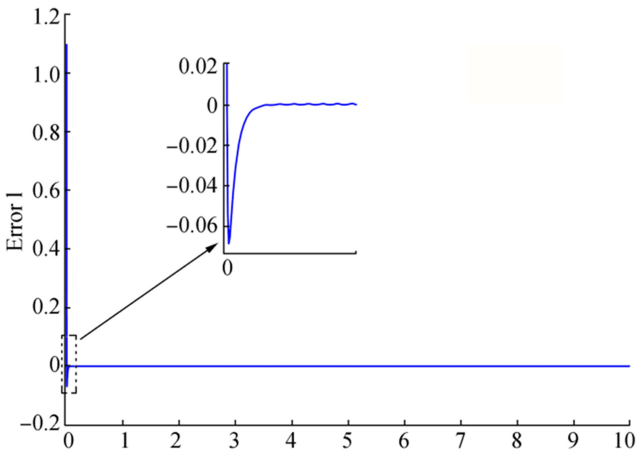

Figure 3 Estimation error of first state (z_1)

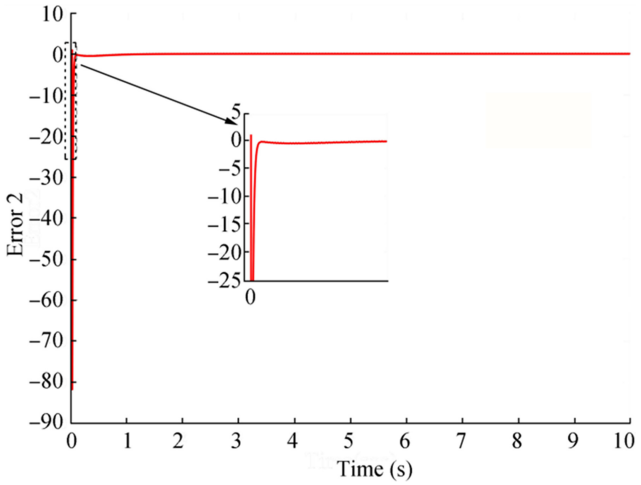

Figure 4 Estimation error of second state (z_2)

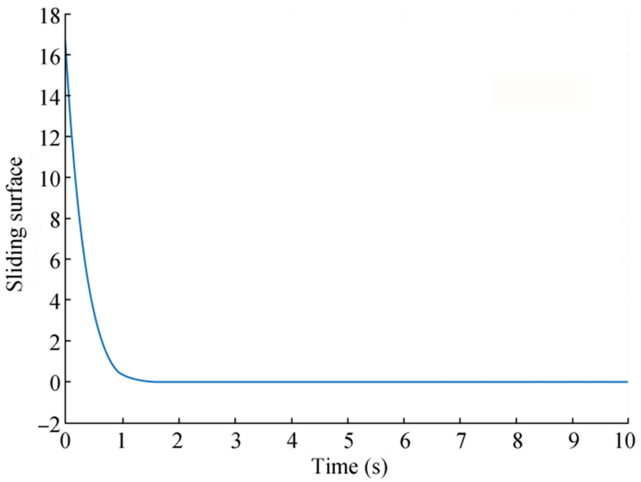

Figure 5 Sliding surface of the terminal sliding-mode controller

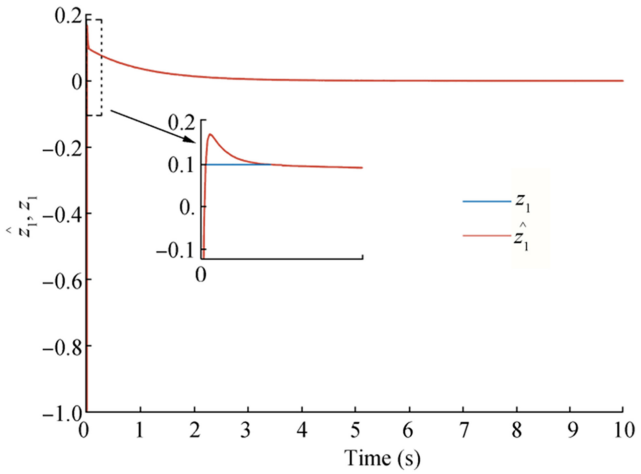

Figure 6 Estimation of z_1 and real z_1

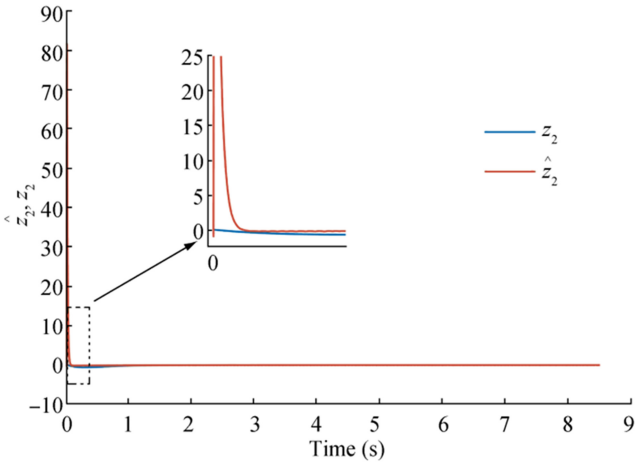

Figure 7 Estimation of z_2 and real z_2

The purpose of the simulation is to demonstrate the stability of the closed-loop system and the estimation accuracy.

The earlier mentioned control laws and observer were applied to the system, and the following results were obtained:

The convergence of the observer estimation error to zero is depicted in Figures 3 and 4. The results show the promising performance of the proposed neuro-observer.

The sliding surface of the terminal sliding-mode controller also converges to zero (Figure 5).

The first state of the system and its estimation are depicted in Figure 6.

The second state of the system and its estimation are depicted in Figure 7.

The convergence of the states and their estimations to the origin demonstrate the asymptotic stability of the closed-loop system in presence of the disturbances.

6 Conclusions

In this paper, a neuro-observer-based robust controller is designed for a class of nonlinear, controllable, and observable systems, and it can say that both classic and intelligent approaches are combined to design an observer-based controller. An adaptive neural network observer with guaranteed stability is derived for the nonlinear dynamics of a hovercraft, which is controlled via a nonsingular super-twisting terminal sliding-mode method. The backpropagation algorithm is applied to update the weighting parameters due to the Lyapunov stability of the overall system. The super-twisting algorithm reduces the chattering phenomenon. Moreover, the Lyapunov stability of the closed-loop system, the convergence of both the tracking and observer errors to zero, and the robustness of the controller against uncertainties and disturbances are all achieved. The simulation results demonstrate the effectiveness of the presented methodology.

References

Abbaspour A, Aboutalebi P, Yen KK, Sargolzaei A (2017) Neural adaptive observer-based sensor and actuator fault detection in nonlinear systems: application in UAV. ISA Trans 67:317–329. https://doi.org/10.1016/j.isatra.2016.11.\

Aguiar AP, Cremean L, Hespanha JP (2003) Position tracking for a nonlinear underactuated hovercraft: controller design and experimental results. 42nd IEEE International Conference on Decision and Control (IEEE Cat. No. 03CH37475), pp 3858–3863

Boiko I, Fridman L (2005) Analysis of chattering in continuous sliding-mode controllers. IEEE Trans Autom Control 50:1442–1446. https://doi.org/10.1109/TAC.2005.854655

Ding F, Meng X, Zhang T (2017) Based on disturbance observer of air cushion vehicle course sliding backstepping control. 2017 IEEE International Conference on Mechatronics and Automation (ICMA), pp 827–832

Duan K, Simon F, Yan Z, Wei S (2018) Artificial neural networks in coordinated control of multiple hovercrafts with unmodeled terms. Appl Sci 8:862. https://doi.org/10.3390/app8060862

Grigoryev V, Rauh A, Aschemann H, Paschen M, 2010. Development of a neural network-based controller for ships. Proc. of the 1st Joint International Conference on Multibody System Dynamics, Lappeenranta, Finland.

Huang J, Mengshi Z, Songhyok R, Caihua X, Zhijun L, Yu K (2019) High-order disturbance-observer-based sliding mode control for mobile wheeled inverted pendulum systems. IEEE Trans Ind Electron 67:2030–2041. https://doi.org/10.1109/TIE.2019.2903778

Hui L, Li J (2009) Terminal sliding mode control for spacecraft formation flying. IEEE Trans Aerosp Electron Syst 45:835–846. https://doi.org/10.1109/TAES.2009.5259168

Jeong S, Eom M, Chwa D (2015) Disturbance-estimation-based hierarchical sliding mode control of hovercraft with wind disturbance. 15th International Conference on Control, Automation and Systems (ICCAS), pp 532–537

Khoygani MRR, Ghasemi R (2016) Neural estimation using a stable discrete-time MLP observer for a class of discrete-time uncertain MIMO nonlinear systems. Nonlinear Dyn 84:2517–2533. https://doi.org/10.1007/s11071-016-2662-z

Kunusch C, Puleston PF, Mayosky MA, Riera J (2008) Sliding mode strategy for PEM fuel cells stacks breathing control using a super-twisting algorithm. IEEE Trans Control Syst Technol 17:167–174. https://doi.org/10.1109/TCST.2008.922504

Lau JY, Liang W, Tan KK (2019) Motion control for piezoelectric-actuator-based surgical device using neural network and extended state observer. IEEE Trans Ind Electron 67:402–412. https://doi.org/10.1109/TIE.2019.2897542

Liang X, Xingru Q, Wang N, Rubo Z, Ye L (2019) Three-dimensional trajectory tracking of an underactuated AUV based on fuzzy dynamic surface control. IET Intell Transp Syst 14:364–370. https://doi.org/10.1049/iet-its.2019.0347

Lin X, Wang L (2017) Heading control of Air Cushion Vehicle with disturbance observer based on terminal sliding mode. 2017 IEEE International Conference on Mechatronics and Automation (ICMA), pp 858–862

Liu W, Li P (2019) Disturbance observer-based fault-tolerant adaptive control for nonlinearly parameterized systems. IEEE Trans Ind Electron 66:8681–8691. https://doi.org/10.1109/TIE.2018.2889634

Liu Z, Li S, Ji Z (2018) Neural network observer-based leader-following consensus of heterogenous nonlinear uncertain systems. Int J Mach Learn Cybern 9:1435–1443. https://doi.org/10.1007/s13042-017-0654-z

Ma Y, Yuanli C, Yu Z (2019) Adaptive neural network disturbance observer based nonsingular fast terminal sliding mode control for a constrained flexible air-breathing hypersonic vehicle. Proc Inst

Mech Eng 233:2642–2662. https://doi.org/10.1177/2F0954410018784824

Marconett AL (2003) A study and implementation of an autonomous control system for a vehicle in the zero drag environment of space. University of California, Davis

Mobayen S, Javadi S (2017) Disturbance observer and finite-time tracker design of disturbed third-order nonholonomic systems using terminal sliding mode. J Vib Control 23:181–189. https://doi.org/10.1177/2F1077546315576611

Mobayen S, Tchier F, Ragoub L (2017) Design of an adaptive tracker for n-link rigid robotic manipulators based on super-twisting global nonlinear sliding mode control. Int J Syst Sci 48:1990–2002. https://doi.org/10.1080/00207721.2017.1299812

Moghanloo D, Ghasemi R (2016) Observer based fuzzy terminal sliding mode controller design for a class of fractional order chaotic nonlinear systems. Int J Eng 29:1574–1581. https://doi.org/10.5829/idosi.ije.2016.29.11b.00

Morales R, Sira-Ramírez H, Somolinos JA (2015) Linear active disturbance rejection control of the hovercraft vessel model. Ocean Eng 96:100–108. https://doi.org/10.1016/j.oceaneng.2014.12.031

Mutreja O, Motwani V, Maru A, Pathak N (2015) Hovercraft with GPS & object detection. Int J Comput Technol Appl 6

Nath A, Dey R, Aguilar-Avelar C (2019) Observer based nonlinear control design for glucose regulation in type 1 diabetic patients: an LMI approach. Biomed Signal Process Control 47:7–15. https://doi.org/10.1016/j.bspc.2018.07.020

Niu Y, Lam J, Wang X, Ho DWC (2004) Observer-based sliding mode control for nonlinear state-delayed systems. Int J Syst Sci 35:139–150. https://doi.org/10.1080/00207720410001671732

Qiu J, Kangkang S, Wang T, Gao H (2019) Observer-based fuzzy adaptive event-triggered control for pure-feedback nonlinear systems with prescribed performance. IEEE Trans Fuzzy Syst 27:2152–2162. https://doi.org/10.1109/TFUZZ.2019.2895560

Rashid MZA, Aras MSM, Kassim MA, Ibrahim Z, Jamali A (2012) Dynamic mathematical modeling and simulation study of small scale autonomous hovercraft. Int J Adv Sci Technol 46:95–114

Resendiz J, Yu W, Fridman L (2008) Two-stage neural observer for mechanical systems. IEEE Trans Circuits Syst 55:1076–1080. https://doi.org/10.1109/TCSII.2008.2001962

Rigatos GG, Raffo GV (2015) Input–output linearizing control of the underactuated hovercraft using the derivative-free nonlinear kalman filter. Unmanned Syst 3:127–142. https://doi.org/10.1142/S2301385015500089

Shah P, Singh B (2019) Adaptive observer based control for roof-top solar PV system. IEEE Trans Power Electron 35:9402–9417. https://doi.org/10.1109/TPEL.2019.2898038

Sharafian A, Ghasemi R (2017) Stable state dependent Riccati equation neural observer for a class of nonlinear systems. Int J Model Identif Control 28:256–270. https://doi.org/10.1504/IJMIC.2017.086570

Sharafian A, Ghasemi R (2019) Fractional neural observer design for a class of nonlinear fractional chaotic systems. Neural Comput & Applic 31:1201–1213. https://doi.org/10.1007/s00521-017-3153-y

Sira-Ramírez H (2002) Dynamic second-order sliding mode control of the hovercraft vessel. IEEE Trans Control Syst Technol 10:860–865. https://doi.org/10.1109/TCST.2002.804134

Soneda Y, Ohtsuka T (2002) Nonlinear moving horizon state estimation for a hovercraft with continuation/gmres method. Proceedings of the International Conference on Control Applications, pp 1088–1093

Tanaka K, Iwasaki M, Wang HO (2000) Stability and smoothness conditions for switching fuzzy systems. Proceedings of the 2000 American Control Conference. ACC (IEEE Cat. No. 00CH36334), pp 2474–2478

Tunstel E, Hockemeier S, Jamshidi M (1994) Fuzzy control of a hovercraft platform. Eng Appl Artif Intell 7:513–519. https://doi.org/10.1016/0952-1976(94)90030-2

Utkin VI, Poznyak AS (2013) Adaptive sliding mode control with application to super-twist algorithm: equivalent control method. Automatica 49:39–47. https://doi.org/10.1016/j.automatica.2012.09.008

Wang N, Ahn CK (2019) Hyperbolic-tangent LOS guidance-based finite-time path following of underactuated marine vehicles. IEEE Trans Ind Electron 67:8566–8575. https://doi.org/10.1109/TIE.2019.2947845

Wang N, He H (2019) Dynamics-level finite-time fuzzy monocular visual servo of an unmanned surface vehicle. IEEE Trans Ind Electron 67:9648–9658. https://doi.org/10.1109/TIE.2019.2952786

Wang C, Liu Z, Fu M, Bian X (2010) Amphibious hovercraft course control based on adaptive multiple model approach. 2010 IEEE International Conference on Mechatronics and Automation, pp 601–604

Wang C, Zhang H, Fu M (2012) Motion control of an amphibious hovercraft based on fuzzy weighting. 2012 IEEE 14th International Conference on Communication Technology, pp 1006-1011

Wang D, Qun Z, Bailing T, Shikai S, Xiuyun Z, Xinyi Z (2018) Neural network disturbance observer-based distributed finite-time formation tracking control for multiple unmanned helicopters. ISA Trans 73:208–226. https://doi.org/10.1016/j.isatra.2017.12.011

Xie W, Cabecinhas D, Cunha R, Silvestre C (2018) Robust motion control of an underactuated hovercraft. IEEE Trans Control Syst Technol 27:2195–2208. https://doi.org/10.1109/TCST.2018.2862861

Zhao B, Xu S, Guo J, Ruimin J, Jun Z (2019) Integrated strapdown missile guidance and control based on neural network disturbance observer. Aerosp Sci Technol 84:170–181. https://doi.org/10.1016/j.ast.2018.10.025

Zhou Q, Peng S, Xu S, Hongyi L (2012) Observer-based adaptive neural network control for nonlinear stochastic systems with time delay. IEEE Trans Neural Netw Learn Syst 24:71–80. https://doi.org/10.1109/TNNLS.2012.2223824